CRREL

(2)

Rotating Multicylinder Method for the Measurement of Cloud Liquid-Water Content and Droplet Size

John B. Howe

January 1991

CRREL REPORT 91-2

For conversion of SI metric units to U.S./British customary units of measurement consult ASTM Standard E380, Metric Practice Guide, *published by the American Society for Testing and Materials, 1916 Race St., Philadelphia, Pa. 19103.*

Cover: Rotating multicylinder in use at Mount Washington Observatory. (Photo by Mark Hitchcock.)

CRREL Report 91-2

U.S. Army Corps of Engineers
Cold Regions Research & Engineering Laboratory

Rotating Multicylinder Method for the Measurement of Cloud Liquid-Water Content and Droplet Size

John B. Howe

January 1991

Prepared for
OFFICE OF THE CHIEF OF ENGINEERS

A-1

PREFACE

This report was prepared by John B. Howe of the Mount Washington Observatory, Gorham, New Hampshire. Report preparation was funded through DA Project 4A161102AT24, *Research in Snow, Ice and Frozen Ground*, Task FS, Work Unit 005, *Concepts of Mesoscale Winter Meteorological Processes*; some of the work described was funded through other CRREL projects during the past 15 years. Other studies by the author discussed in this report were funded by USAF Air Materiel Command, Sigma Xi, and the National Science Foundation.

Many past and present staff members of the Mount Washington Observatory and of the Aeronautical Icing Research Laboratories have been involved in gathering the data for the many hundreds of Rotating Multicylinder exposures that the author has analyzed or examined. Other individuals whose counsel has been influential include R. Cunningham, formerly of Air Force Cambridge Research Laboratories; W. Howell, formerly of the Mount Washington Observatory; P. Perkins, formerly of the National Advisory Committee for Aeronautics/National Aeronautics and Space Administration; and C. Franklin, formerly of the Aeronautical Icing Research Laboratories. The support and advice of S. Ackley, J. Govoni, K. Jones, C. Ryerson, and W. Tucker of CRREL are gratefully acknowledged.

CONTENTS

ILLUSTRATIONS

TABLE

NOMENCLATURE

a	droplet radius (cm)
C	cylinder diameter (cm)
D	droplet diameter (μm)
E	collection efficiency, dimensionless
E_M	overall weighted collection efficiency
f_1	$9(V/\eta)\,(\rho_a)^2$
K	inertia parameter, $\frac{\rho_w D^2 V}{9\eta C}$, dimensionless
L	length of ice collection (cm)
LWC	liquid-water content (g/m^3) (informal usage)
N_{Re}	free-stream Reynolds number with respect to droplet diameter, $\rho_a DV/\eta$, equivalent to $(K\phi)^{1/2}$
T	exposure duration (s)
V	free-stream airspeed (cm/s)
W	liquid-water content (g/m^3)
w	cylinder weight (g)
η	absolute viscosity of air (g/cm s)
ρ	density (g/cm^3)
ϕ	$\frac{(N_{Re})^2}{K} = \frac{9\rho_a^2 CV}{\rho_w \eta}$, dimensionless

Subscripts

a	air
av	average
d	volume median
i	with ice collection
o	without ice collection
w	liquid water

Rotating Multicylinder Method for the Measurement of Cloud Liquid-Water Content and Droplet Size

JOHN B. HOWE

INTRODUCTION

The Rotating Multicylinder (RMC) method has been in use since the late 1940s, but no description of it has ever appeared in the open literature, although it is among the best, and is certainly the simplest and most reliable, of any technique for the measurement of cloud liquid-water content and droplet size in icing conditions. This report attempts to provide sufficient information to enable someone unfamiliar with the method to build and use the instrument. Included also is a review of the theory upon which the data analysis procedure is based.

HISTORY

The RMC method was developed at the Mount Washington Observatory (MWO) between 1940 and 1945 after prior use of a single rotating collector for measuring liquid-water content (LWC) of clouds (Arenberg 1939, 1941). The method was given a rigorous theoretical basis by Langmuir (1944) and Langmuir and Blodgett 1946). Langmuir (1944) mentions some prior work by F. Albrecht in Germany and by M. Glauert in England. Other workers involved in the development of the method at the MWO included V. Clark of the MWO staff, R. Cunningham of MIT, and V. Schaefer of General Electric. During the late 1940s and the 1950s the method was used extensively for icing studies in natural wind, wind tunnels, and aircraft by various groups, including the National Advisory Committee for Aeronautics (NACA), the Aeronautical Icing Research Laboratories (AIRL), and the MWO. Tabulations of data collected with the method appeared in a series of quarterly reports by the MWO staff (1949–51). Ambrosio (1950) tabulated all results obtained by all agencies during the period 1945–1950, a total of some 3600 observations.

METHOD

General description

A cylinder exposed for a known period of time in an airstream, with its axis perpendicular to the flow, will "sweep out" a known volume of air. If the air contains droplets of supercooled water, it might be assumed that all the droplets in the swept-out volume would strike and freeze on the cylinder. This assumption is nearly correct when the droplets are very large and/or the airspeed is very high. However, as the droplet size or airspeed becomes smaller the droplets have less momentum, and those near the edges of the swept-out volume will tend to follow the airstream lines around the cylinder without striking it. If the diameter of the cylinder is increased, this effect becomes more pronounced. The ratio of the mass of liquid water striking the cylinder to the total mass of liquid water in the swept-out volume is called the collection efficiency E of the cylinder. Collection efficiency varies directly with airspeed and droplet size and inversely with cylinder diameter. Collection efficiency is affected to a smaller degree by changes in the density and viscosity of the air.

The liquid-water content of a cloud (LWC for informal usage, W in mathematical usage) is the mass of liquid water per unit volume. The mass of ice collected on a cylinder per unit of swept-out volume is equal to the LWC of the cloud multiplied by the collection efficiency of the cylinder, or EW. In practice, EW for a cylinder is calculated from the relation

$$EW = \frac{\text{weight of collected ice}}{\text{swept-out volume}}$$

where the swept-out volume is calculated from measured values of airspeed, exposure duration, cylinder length, and average cylinder diameter. (Average diameter is the mean of the diameters at the beginning and end of the exposure, the cylinder having been rotated during exposure to produce a cylindrical ice collection.)

In the RMC method, several cylinders of different diameters are exposed simultaneously; the resulting ice collections are measured and the values of cylinder diameter vs *EW* are plotted on logarithmic paper.

Theoretical studies of droplet trajectories near cylinders have resulted in graphs of a dimensionless parameter $1/K$ vs cylinder collection efficiency; the experimental data plot is fitted to one of these curves, LWC is read off directly, and a simple calculation yields the droplet diameter.

Instrumentation

Figure 1 shows an instrument assembled and disassembled; working drawings and a detailed description are given in Appendix A. Many other designs have been used, but this one is the simplest for natural wind. The diameter of the cylinders is not critical and standard aluminum tubing sizes may be used such that each cylinder is approximately twice the diameter of its smaller neighbor. A slightly loose fit between all components makes for ease of disassembly.

The bottom end of the shaft is threaded to fit the drive motor shaft. At MWO we use gear motors giving about 1 or 2 rpm; rotation speed should be close to this range, but is not critical. (Aircraft speeds require faster rotation.) We have several taper mounts on our tower railing so that the drive motor with the RMC can be exposed on whatever happens to be the windward side. Provision may have to be made for adjusting the angle of the motor mount so that the instrument shaft is perpendicular to the wind vector. Before any exposures are made, the site should be checked with a straight rod collector to assure

a. Assembled.

Figure 1. Rotating multicylinder instrument.

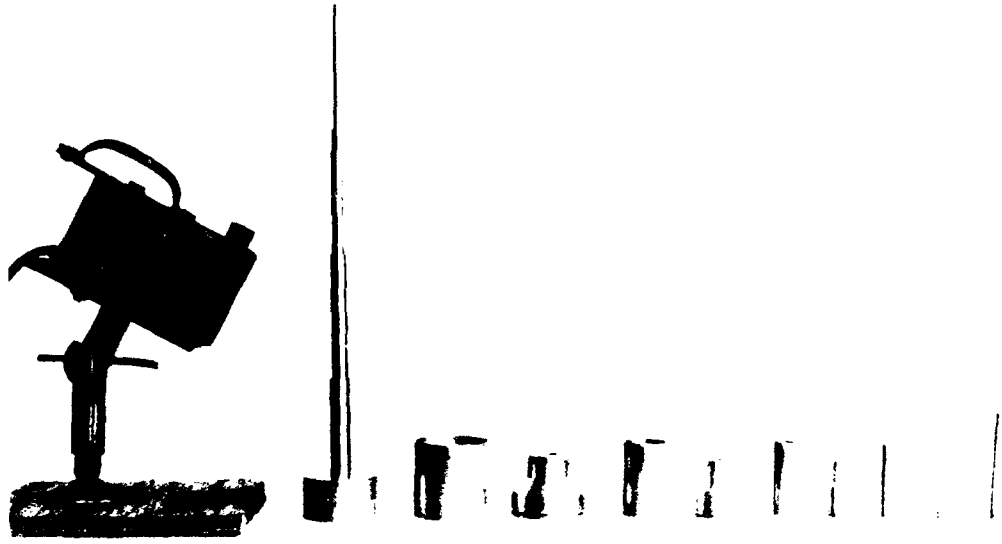

b. Disassembled.
Figure 1 (cont'd).

that the instrument will be outside the boundary layer with uniform impingement along the collector.

Wind speed must be measured as accurately as possible. We are fortunate in that the MWO official anemometer is a heated, vane-mounted Pitot-static tube. If an anti-iced anemometer is not available, an accurate cup anemometer can be used if it is put in place just before the beginning of an RMC run, since the small amount of ice or rime that collects on the cups during the exposure should not be detrimental.

Weighing (to ±0.01 g), length measurement (to ±0.05 cm), and timing (normally to ±5 s) require no special equipment. Ice diameter is most easily measured with a micrometer caliper. Care must be taken not to depress the rime surface when measuring a diameter: the caliper must be adjusted by eye, not by feel. For the three largest cylinders this measurement is most easily done by measuring one side of the iced cylinder over an anvil. (A device for this is easily made by inserting a length of 2-mm wire vertically into a small piece of plywood.)

Exposure procedure

A step-by-step outline of exposure and data-reduction procedure is given in Appendix C.

On Mt. Washington we make exposures in natural winds ranging from ~30 to ~150 km/hr. For the higher speeds of aircraft it may be advisable to use larger cylinder diameters; for ground sites with winds of less than 30 km/hr it may be necessary to employ a carefully designed small wind tunnel.

The instrument must be at a subfreezing temperature prior to the beginning of an exposure. Exposure durations in Mt. Washington conditions range from 5 to 40 minutes. Our rule of thumb is to end an exposure when the collection on the smallest cylinder has reached approximately the original diameter of the no. 2 cylinder. This is a compromise between the desire to minimize percentage weighing errors and the need to maintain the spread in cylinder diameters. Disassembly and measurement after the exposure is usually a straightforward, albeit rather delicate, job, but when hard clear ice is collected it helps to have a warm cutting tool. (A light bulb in an open-ended tin can with sheet copper blades soldered to one end is ideal.) Disassembly and length and diameter measurement must be done in a coldroom. Weighing will usually be done at the same time, but if this is inconvenient the iced cylinders can be stored in canisters for later weighing. If part of the collection on a cylinder is accidentally broken off, the remaining ice can be trimmed to give a "square" end; the length dimension required is, of course, that of the ice, not that of the cylinder itself.

Data reduction—preliminary

Several quantities must be computed prior to the curve-matching step:

1. Average diameter (C_{av}, cm) for each cylinder, the mean of the iced and bare diameters.

2. Product of LWC and collection efficiency (EW) for each cylinder:

$$EW = \frac{w_i - w_o}{VLTC_{av}} \times 10^6, \text{ g/m}^3. \quad (1)$$

3. Air density (ρ_a)

$$\rho_a = \frac{0.348 \text{ (pressure [mb])}}{\text{(temperature[K])}} \times 10^{-3}, \quad \text{g/cm}^3. \quad (2)$$

4. Airspeed divided by viscosity (V/η)

$$\frac{V}{\eta} = \frac{V}{2.48 \text{ (temp[K])}^{0.754}} \times 10^6, \frac{\text{cm/s}}{\text{g/cm s}}. \quad (3)$$

5. An intermediate factor (f_1)

$$f_1 = 9(V/\eta)(\rho_a)^2. \quad (4)$$

The values of C_{av} are then plotted vs EW on three-cycle logarithmic tracing paper (Fig. 2).

Data reduction—curve matching

The theoretical curves, to which we fit the plots of C_{av} vs EW, are graphs of a dimensionless parameter ($1/K$) vs cylinder collection efficiency (E_M), drawn for selected values of $K\phi$. ($K\phi$ is a dimensionless parameter equal to the square of the Reynolds number for the volume-median droplet size.) For each value of $K\phi$ there is a family of curves labeled "A" through "J" ("I" is omitted). The "A" curves assume all droplets are the same size, while the others assume progressively broader droplet size distributions. The curves must be drawn on the same type of graph paper used for plotting the data points. It is convenient to put all nine curves of each family on one sheet of paper, with the vertical axis shifted slightly for each curve. A small inverted T marks the point $1/K = 1$, $E = 1$ for each curve. An example of these curves is shown and the theory of their use is described and explained more fully in Appendix B.

The matching of the C_{av} vs EW plot to the theoretical curves must be done using a curve whose $K\phi$ value is closest (on a logarithmic scale) to the actual value for the exposure being analyzed; this value is of course not known a priori, since $K\phi$ is a function of droplet size. Therefore, one must make a guess and try, e.g., the $K\phi = 200$ family. (After some experience one's first guess will usually turn out to be correct.) The procedure is as follows:

1. Slide the graph paper with your plotted points around on the theoretical curves, keeping the axes parallel, until you find the best match.

2. Read on your plotted graph the value of C_{av} which lies over the $1/K = 1$ axis of the theoretical curve; this is the value of cylinder diameter for which $K = 1 (C_{K=1})$ for the conditions of this exposure.

3. Multiply this number times the value of f_1 (previously determined by eq 4) to find the value of $K\phi$. If this is closer, on a log scale, to 200 than it is to 20 or 1000 you have used the correct family of curves; if not, repeat the matching process using the appropriate family.

4. Trace the curve lightly, and trace the corresponding inverted T.

5. Now read the value of LWC for your exposure on the horizontal scale of your plot over the $E_M = 1$ axis of the theoretical curve (in line with the inverted T).

6. Use the value of C_{av} for which $1/K = 1$ to compute the volume-median droplet diameter (D_d) and $K\phi$:

$$D_d = \left[9\left(\frac{\eta}{V}\right)C_{K=1}\right]^{1/2} \times 10^4, \ \mu m \quad (5)$$

$$K\phi = f_1(C_{K=1}). \quad (6)$$

See Figure 2 for examples of curve matching for exposures made on Mt. Washington. Figure 2a is from a run for which a mistake was made in the measurement of the no. 3 cylinder; the effect of the mistake is obvious and easily allowed for. Figure 2b is typical of runs made when wind speed is low and/or D_d is small; there was only a dusting of rime on the two largest cylinders, which were not measured, and the no. 4 cylinder had a slightly spotty collection. In such cases points for cylinders with spotty collections are best ignored, even though it may be possible to achieve an approximate fit of all the points to a theoretical curve of narrower distribution. Figure 2c illustrates the opposite set of conditions, with high wind speed and large D_d. A step-by-step explanation of the exposure and analysis procedure is given in Appendix C.

Computer processing

All the computations described above can be done by a very simple computer program; with a hand calculator they can be done almost as easily. Attempts have been made to computerize the curve-matching process, but in my opinion this is a mistake. Aside from considerations of questionable cost-effectiveness, "wrong" matches, due to measurement errors or spotty collections, may result and will be difficult or impossible to detect. A strong recommendation for the method described in the preceding sections is that such errors can usually be recognized before they do any damage.

Use of method in warm fog

The RMC can be used in above-freezing temperatures if the cylinders and intercylinder adapters are made of a porous material; it may be simpler to wrap the regular metal parts in a porous substance such as Millipore filter material. Weights must be measured before as well as after each exposure, and great care is needed

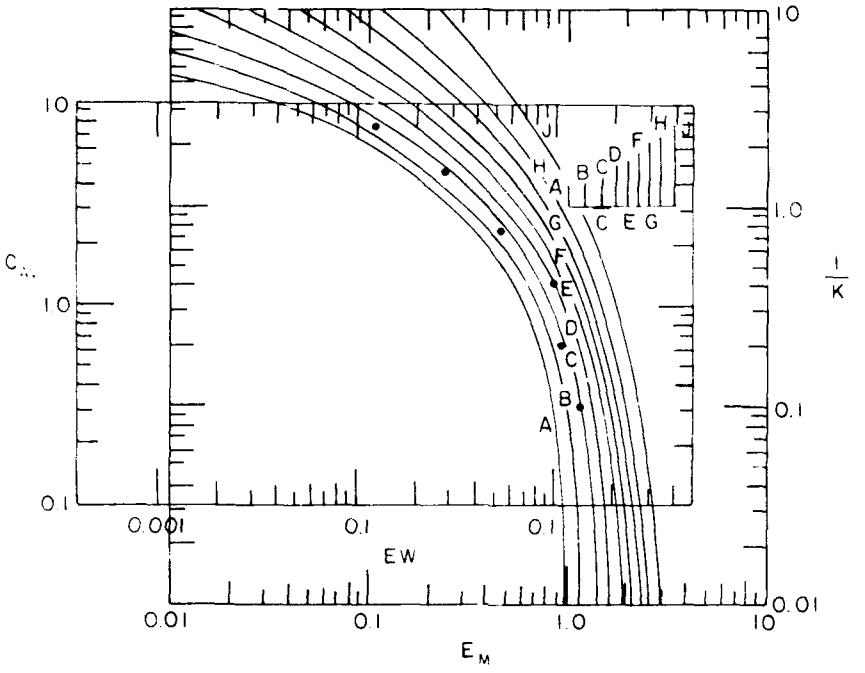

a. Run for which a mistake was made in measurement of the no. 3 cylinder ($W = 0.17$ g/m^3, $C_{(K=1)} = 2.9$, $D_d = 12$ μm).

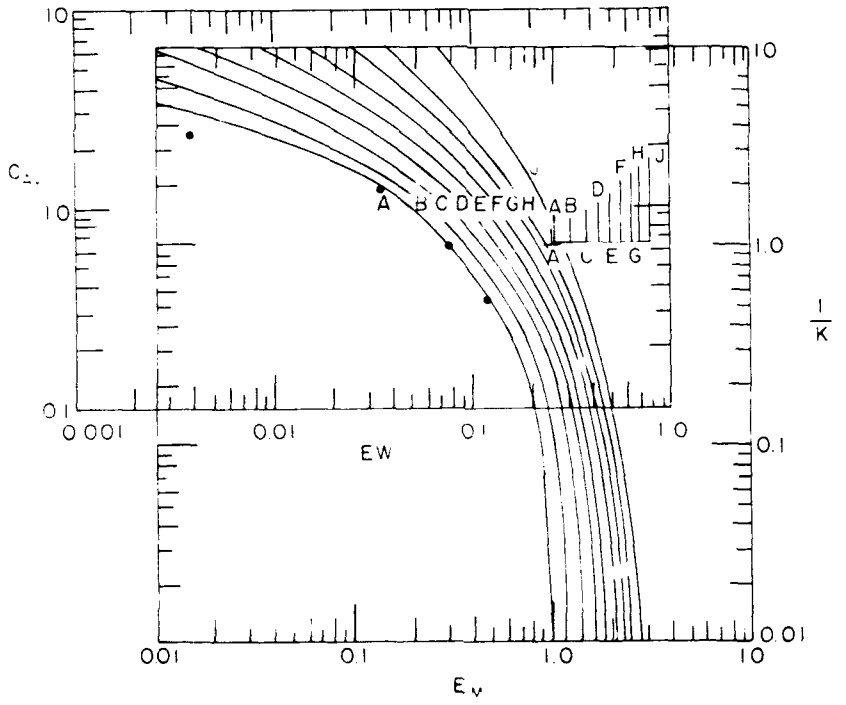

b. Tyical run with low wind speed and or small D_d ($W = 0.25$ g/m^3, $C_{(K=1)} = 0.64$, $D_d = 5$ μm).

Figure 2. Examples of curve matching.

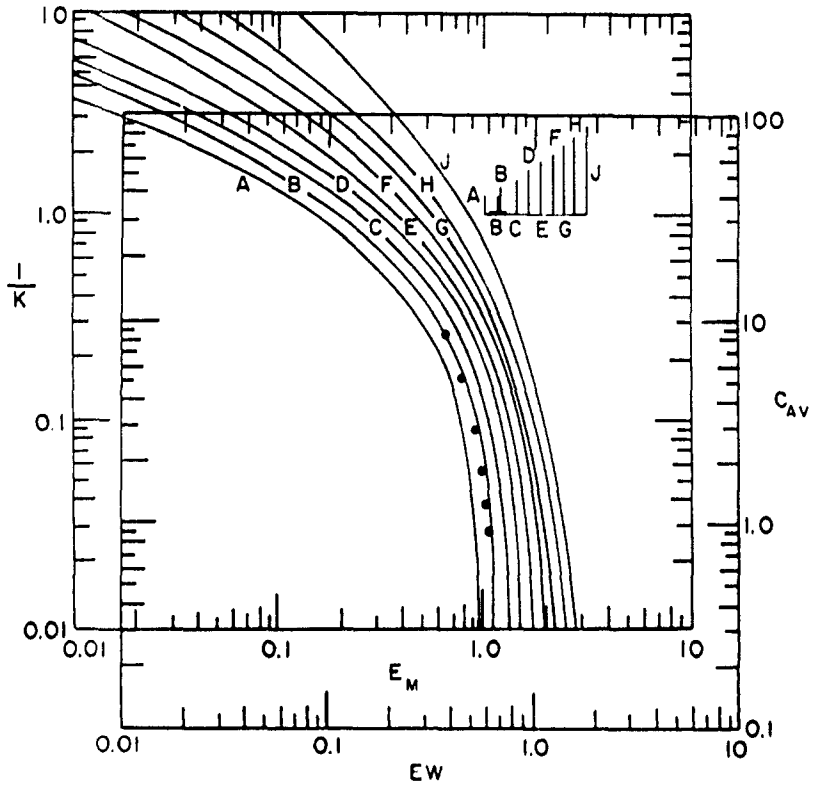

c. Typical run with high wind speed and large D_d *(*$W = 0.68\ g/m^3$, $C_{(K=1)} = 33.0$, $D_d = 39\ \mu m$*).*

Figure 2 (cont'd). Examples of curve matching.

to ensure that the cylinders (particularly the smaller ones) do not become saturated.

DISCUSSION OF ACCURACY

This discussion will begin by considering the accuracy of an "ideal" exposure resulting in complete coverage of at least five cylinders. (Ideal exposures are actually quite common, comprising perhaps half of all runs made at MWO.) Following this we will consider, first, conditions that may result in reduced accuracy, and then discuss hidden problems due to possible errors in the theoretical curves. Finally we will briefly review the results of comparison tests, both between RMCs and between the RMC and other instruments.

"Ideal" runs

If the physical measurements have been made with reasonable care, the plotted data points should all be within 5% of their true locations. (The most likely source of greater error is in the measurement of wind speed.)

An ideal exposure will result in an almost perfect curve match; if the curve is similar to that of Figure 2a accuracy in W and D_d will be comparable to that of the original measurements, except that errors in wind speed measurement have a smaller effect on the computed D_d (eq 5). If the overall slope of the curve is low, as in Figure 2b, accuracy in W will be somewhat lower because there is less constraint on the "sideways" position during matching. For cases like Figure 2c, with a steeply sloping plot, accuracy in D_d will be lower because there is less constraint on the "up-and-down" position.

Errors due to carelessness in measurement or to breakage of ice will inevitably occur, but will rarely affect more than one or two cylinders. Such errors can usually be easily recognized in the data plot and allowed for during curve matching, so accuracy will not be seriously affected (Fig. 2a).

Thus for ideal runs, assuming the validity of the theoretical curves, accuracy in W and D_d is estimated to be ±10% or better. This includes the effect of small errors caused by the actual value of $K\phi$ being different from the value used to construct the theoretical curve.

"Non-ideal" runs

When D_d is very small and/or wind speed is low, the larger cylinders may have a spotty collection (individual kernels of rime) or no collection at all. Figure 2b,

referred to in a previous section, shows an example of this. Sometimes there will be measurable collections on only three cylinders, rarely on only two. This has a potentially drastic effect on accuracy, especially since a measurement error on one of the cylinders cannot be detected in the data plot.

The plotted points for cylinders with spotty collections tend to fall below the proper theoretical curve. Though they can often be forced into an approximate fit by going to a curve for a narrower distribution, such a forced fit will be of questionable validity. A notation should always be made on the measurement work sheet when collections are spotty, even when coverage is near 100%, and the data points for any spotty cylinders must be treated with suspicion during curve matching. In these cases the reduction in accuracy can range from insignificant to serious and will have to be judged case by case. It is helpful to include with the analysis results for each run a notation as to the number of points that fit the theoretical curve within approximately 5%.

Runoff

Moderate temperatures and/or high rates of water impingement can result in some fraction of the collected water running off without freezing; the smaller cylinders are most likely to be affected. The collection will be of clear ice, although the occurrence of clear ice does not necessarily indicate runoff. If possible, the instrument should be checked visually during exposure when there is any likelihood of this phenomenon; it is usually easy to see.

Exposures with runoff will of course yield only a "lower limit" value of LWC and a very unreliable value of D_d, even if accurate measurement of the (usually rapidly melting) ice is possible.

Accuracy of theoretical curves

The preceding discussion assumed that the theoretical curves are accurate. Is this assumption valid? The droplet trajectory analysis upon which the curves are based was done originally for an incompressible flow field with the differential analyzer at the General Electric Research Laboratory (Langmuir and Blodgett 1946). This analysis was redone for a compressible flow field by NACA, using a mechanical analog based on the differential analyzer (Brun et al. 1955). The NACA results were slightly different, and NACA also improved the method for computing the RMC curves. We use the NACA data and computation method. The trajectory analysis was repeated on a computer by McComber and Touzot (1981) using the method of finite elements. Their work confirmed the accuracy of the NACA results; there were some differences, but these would not alter the RMC curves significantly. Although some uncertainty may remain regarding the effects of turbulence and of cylinder surface roughness, there is a high degree of confidence in the accuracy of the RMC curves for monodisperse droplet populations.

A fundamental and potentially serious problem remains, however, concerning the development of the curves for the B through J droplet size distributions. Langmuir's original method has, to my knowledge, been used in all subsequent work. (My own attempts at revision will be described below.) Langmuir adopted one of Houghton and Radford's (1938) measured distributions of fog droplet size as a reasonable basis for what he defined as the B distribution; his distributions C, D, and E were derived mathematically therefrom, and the broader distributions were added by the MWO using the same procedure. These distributions are approximately normal (Gaussian), and can be represented as histograms of total droplet volume vs droplet diameter for equal increments of droplet size.

It was recognized during the first seasons of routine RMC exposures at the MWO that bimodal distributions must occasionally occur, particularly during episodes of fog with freezing drizzle or rain. Theoretical curves representing some hypothetical bimodal distributions were produced (these generally recurve, becoming concave upwards for the higher values of $1/K$), but these curves were not found to be very useful. No doubt this attempt failed simply because the possible variations in nature of such bimodal distributions are practically infinite.

I approached this problem in the early 1960s by synthesizing sets of data points for RMC exposures in hypothetical bimodal and trimodal clouds. In all but one of the seven cases studied, the synthesized data points could be fitted to one of the standard theoretical curves. Table 1 summarizes these results. Note that in all but the third case the resulting value of LWC is within 10% of the sum of the LWCs in the synthesized populations, and the resulting volume median droplet diameter and distribution are at least reasonable.

During the 1970s the MWO made a series of simultaneous exposures with the RMC, the Blau Optical Cloud Particle Spectrometer (OCPS) (Ryan et al. 1972), and an oiled-slide droplet collector. (Results of these tests are summarized in a later section.) The raw data from the latter two instruments were in the form of droplet counts, and histograms in most cases showed an approximately normal or Gaussian distribution of droplet count over the range of droplet size. This result was unexpected; whether or not it was entirely correct, it at least strongly suggested that the Houghton/Langmuir distributions, approximately normal with respect to droplet *volume*, might not be representative of conditions in the real world.

Table 1. Synthesized RMC data.

Droplet populations, synthesized data									*Results using standard procedure*		
	I			*II*			*III*				
LWC	D_d	*Dist.*	*LWC*	D_d	*Dist.*	*LWC*	D_d	*Dist.*	*LWC*	D_d	*Dist.*
0.1	8	A	0.2	40	A	—	—	—	0.27	32	F
0.1	8	D	0.1	40	D	—	—	—	0.19	19	J
0.1	8	D	0.3	100	D	—	—	—	0.31	90	E
0.1	8	A	0.1	20	A	0.2	40	A	0.38	25	E
0.1	8	D	0.03	40	D	—	—	—	0.15	9	J
0.1	8	D	0.03	100	D	—	—	—	(0.12)	Poor Fit	
0.2	20	B	0.03	100	B	—	—	—	0.23	23	D

I therefore constructed new sets of theoretical curves with a distribution scheme based on a typical OCPS exposure. For the past 14 years most RMC runs made at the MWO (several hundred runs) have been analyzed on both the new and the old (NACA/Langmuir) curves. In every case, there was very little difference in goodness of fit. Results generally differed by less than 5% in LWC and D_d for narrow and medium distributions; with broad distributions differences were usually less than 10%, but occasionally as much as 20%. The new curves usually, but not always, gave higher values. Indicated distributions were always broader with the new curves, as would be expected.

The two investigations described above show that the RMC method is insensitive to the details of droplet size distribution. The fact that a data plot fits a particular theoretical curve does not imply that the cloud had the size distribution assumed for the curve, and it may in fact have been quite different. *The method gives only a general indication of the breadth of droplet size distribution.* Fortunately, however, this shortcoming has a rather small effect on the accuracy of LWC and D_d values except when the distribution is very broad.

Comparison tests

Howell (1952) investigated the performance of three RMC instruments that differed in several design details, and found no significant differences in results. I did a few such tests with two instruments in 1985, with the same conclusion.

The simultaneous exposures of RMC, OCPS, and an oiled-slide collector, mentioned above, showed reasonably good correlation in D_d, with OCPS values approximately 20% higher than RMC values. This may be partly explained as being due to the presence during most runs of snow or blowing snow, which affected the OCPS but not the RMC. The OCPS gave LWCs that were usually half to one-tenth of those given by the RMC; no explanation for this was found despite much effort. No attempt was made to compute LWC from the oiled-slide data.

Simultaneous exposures of the RMC and the Particle Measuring Systems Forward Scattering Spectrometer Probe (FSSP) at the MWO during 1984–85 gave similar results, i.e., fairly good agreement in D_d, but FSSP values of LWC that were much too small.

The large discrepancies in LWC values are certainly due to poorly understood errors in the optical probes' sensing and/or data processing. This statement sounds arbitrary, but consider the following:

1. RMC physical measurements are straightforward and unlikely to be in error by more than 10%.

2. Even if all the arguments given in preceding sections are disregarded for accuracy of RMC data analysis methods, the *EW* value measured for the smallest cylinder represents a lower limit for the value of LWC. The smallest-cylinder *EW* values for these runs were generally 60% to 80% of the LWC values.

It should be mentioned that both optical probes were calibrated immediately prior to the MWO tests. The calibration of the OCPS was checked immediately after the tests and found to be unchanged.

CONCLUSIONS

The Rotating Multicylinder (RMC) is a low-cost, simple, reliable instrument. Exposure and data-reduction procedures are straightforward; they are somewhat time-consuming, but the almost total lack of maintenance and repair requirements largely offsets this disadvantage. Although intended for use in supercooled clouds, the method can, with some modifications, be used in above-freezing temperatures. With reasonable care in making the necessary physical measurements, accuracy in determination of liquid-water content and droplet size is better than ±10% when cloud droplet-size distribution is narrow or moderately broad. For extremely broad distributions, accuracy may be reduced to about ±20%. The method is insensitive to details of size distribution, but it reliably indicates the approximate distribution breadth.

This accuracy is achieved partly because the method samples an astronomically large number of droplets over a large volume of cloud. This may be a disadvantage in some applications.

Errors in measurement will generally be revealed during data reduction and can easily be allowed for; in most such cases accuracy will not be reduced. Accuracy is worst when the temperature is a few degrees below freezing, due to difficulties in handling and the likelihood of runoff.

LITERATURE CITED

Ambrosio, A. (1950) *Statistical Analysis of Meteorological Icing Conditions*. Los Angeles, California: University of California, Department of Engineering.

Arenberg, D.L. (1939) Riming measurements on Mt. Washington. *Mt. Washington Observatory News Bulletin*, no. 5.

Arenberg, D.L. (1941) Riming program for 1940. *Mt. Washington Observatory News Bulletin*, no. 8.

Brun, R.J., W. Lewis, P.J. Perkins and J.S. Serafini (1955) Impingement of cloud droplets on a cylinder and procedure for measuring liquid-water content and droplet sizes in supercooled clouds by rotating multicylinder method. National Advisory Committee for Aeronautics Report 1215.

Houghton, H.G. and W.H. Radford (1938) On the measurement of drop size and liquid-water content in fogs and clouds. In *Papers in Physical Oceanography and Meteorology*, vol. 4. Massachusetts Institute of Technology–Woods Hole Oceanographic Institute.

Howell, W.E. (1952) Comparison of three multicylinder icing meters and critique of the multicylinder method. National Advisory Committee for Aeronautics Technical Note 2708.

Langmuir, I. (1944) Supercooled water droplets in rising currents of cold saturated air. In *The Collected Works of Irving Langmuir*. New York: Pergamon Press, vol. 10, p. 199–334 (1961).

Langmuir, I. and K.B. Blodgett (1946) A mathematical investigation of water droplet trajectories. In *The Collected Works of Irving Langmuir*. New York: Pergamon Press, vol. 10, p. 335–393 (1961).

McComber, P. and G. Touzot (1981) Calculation of the impingement of cloud droplets in a cylinder by the finite element method. *Journal of Atmospheric Sciences*, **38**: 1027–1036.

Ryan, R.T., H.H. Blau, Jr., P.C. von Thuna, M.L. Cohen and G.D. Roberts (1972) Cloud microstructure as determined by an optical cloud particle spectrometer. *Journal of Applied Meteorology*, **11**: 149–156.

Staff, Mt. Washington Observatory (1949–51) Contributions to the theory of the constitution of clouds. (Reports under Air Force Cambridge Research Laboratory contracts).

APPENDIX A: MULTICYLINDER INSTRUMENT DESIGN

The shaft of the RMC should be made of stainless steel or brass and the cylinders and intercylinder adaptors of aluminum, except for the two smallest cylinders, which may more easily be made of brass. The diameter of the cylinders is not critical; standard tubing sizes can be used such that each cylinder is approximately twice the diameter of its smaller neighbor and the diameter of the largest is about 3 in. (7.62 cm).

A slightly loose fit between all the components makes for ease of disassembly. The bottom adaptor is secured to the shaft with epoxy. The no. 2 cylinder has a flange and threaded lower end, and screws into the top end of the shaft to hold everything in place. The smallest cylinder fits into a drilled hole in the top of the no. 2 cylinder.

Figure A1 shows the design for the shaft and adaptors. Dimensions are given in English units for simplicity; in the U.S. it will be easiest to obtain the tubing for the cylinders in standard inch dimensions. Note that dimensions A and F for the adaptors are equivalent to the associated cylinder diameters, and that B and E will depend on the wall thickness of the tubing used for the cylinders. The flanges shown on the adaptors are optional; our experience is that they do no harm and are helpful at times during disassembly. They influence the ice collection only if the RMC axis is not perpendicular to the airstream, and in fact provide a very sensitive indication of that undesirable condition.

At the MWO our no. 2 cylinder is machined from solid brass rod. Finished length is 11 cm, diameter ~0.5 cm. The bottom 1 cm is threaded to fit the tapped hole in the top of the shaft with a small flange ~0.6 cm in diameter to bear against the top of the II/III adaptor. Our no. 1 cylinder is just a piece of 0.158-cm brass wire about 10 cm long; the bottom end can be crimped slightly so that it fits easily but securely in the drilled hole at the top end of the no. 2 cylinder. The four largest cylinders are made from aluminum tubing with ends machined to give a length of 7.4 cm.

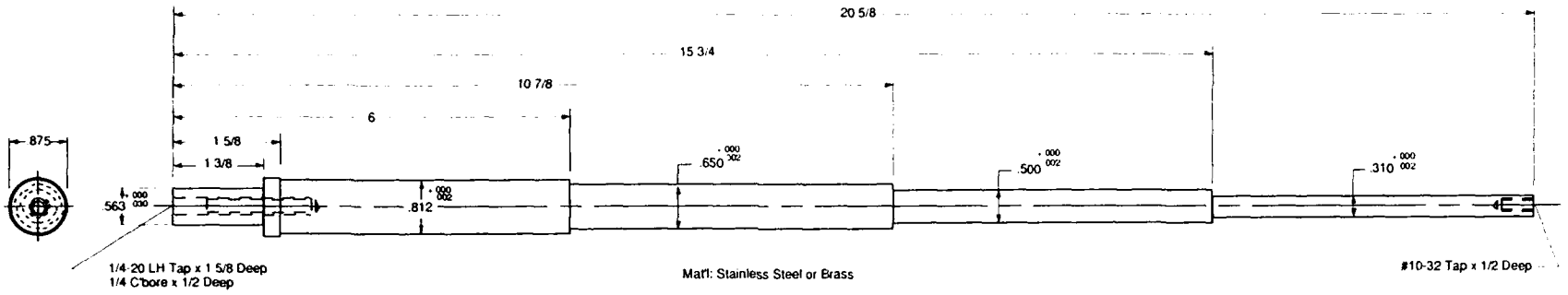

SHAFT

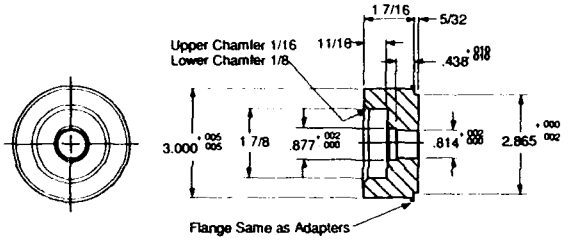

BASE

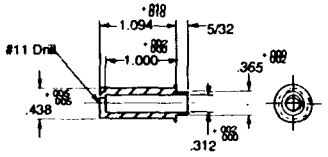

II / III ADAPTER

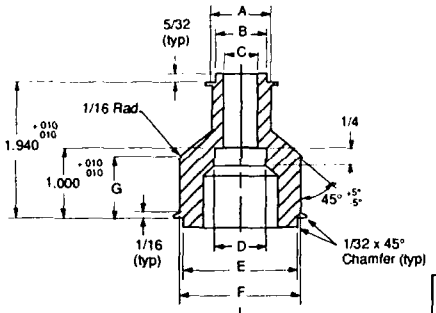

NOTES: Flange Dia. = "A" or "F" dia. plus 1/8.
Counterbore bottom 'ad lib', leaving wall thickness of 1/4 to 3/8.

Diameter	Adaptors III/IV	Adaptors IV/V	Adaptors V/VI
A	0.438 ±0.005	0.875 ±0.005	1.750 ±0.005
B	0.365 +0.000 −0.002	0.757 +0.000 −0.002	1.632 +0.000 −0.002
C	0.312 +0.002 −0.000	0.502 +0.002 −0.000	0.652 +0.002 −0.000
D	0.502 +0.002 −0.000	0.652 0.002 −0.000	0.814 +0.002 −0.000
E	0.757 +0.000 −0.002	1.632 +0.000 −0.002	2.805 +0.000 −0.002
F	0.875 ±0.005	1.750 ±0.005	3.000 ±0.005
G	1.060 ±0.030	0.875 ±0.030	0.690 ±0.030

Figure A1. Instrument design drawings (inches).

APPENDIX B: THEORETICAL CURVES

Droplet size distributions

The droplet size distributions assumed for the theoretical curves are listed in Table B1. These are the same distributions assumed in Langmuir and Blodgett (1946) and in Brun et al. (1955), except for the addition of the broader types, F, G, H, and J.

In Table B1 the droplets in each distribution type are divided into seven groups representing symmetrical subdivisions of the area under the distribution curve. The values a/a_d are the ratios of the droplet radius for each size group to the radius of the volume-median size. The volume fraction of liquid water in each size group is listed in the left column. For the A distribution all the droplets are the same size. The values of a/a_d for the B distribution are raised to the 1.5, 2.0, 2.5, 3.0, 3.5, 4.0, and 5.0 power to obtain the a/a_d values for the C, D, E, F, G, H, and J distributions, respectively.

Calculation of curves of $1/K$ vs E_M

The theoretical curves of $1/K$ vs E_M shown in Figure B1 are constructed from the values given in Table B3. The method of Brun et al. (1955) was used to calculate these values; they gave tables of values for $K\phi = 0$, 200, 1000, 3000, and 10,000 and distributions A through E, which are reproduced here as part of Table B3. The remaining values were calculated by me at the Aeronautical Icing Research Laboratories in 1956. At that time I also calculated values for $1/K = 10.0$ for all $K\phi$ values and distributions where necessary to carry the curves to the top edges of the graphs. (This was not done by Brun et al.).

Values for each of the A curves are calculated by assigning a series of values to $1/K$ and finding the corresponding values of E from the curves of E vs K, with ϕ as a parameter given by Brun et al. (The value of ϕ is determined for each value of $1/K$, since $K\phi$ is held constant for each curve of $1/K$ vs E_M.).

For the B through J distributions of Table B3, overall weighted collection efficiencies (E_M) are used. Table B2, which shows the procedure for finding a single point of the $K\phi = 100$- J distribution curve, will serve as an example. Here the assigned value of $1/K$ is 0.01 (K for volume-median size equals 100, $\phi = 10$). For each size group, the appropriate value of K is found by multiply-

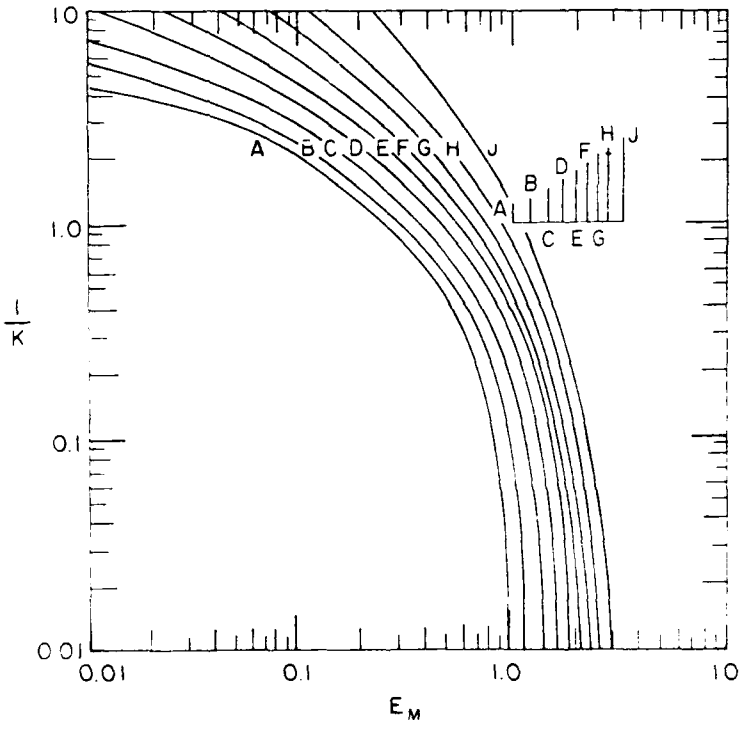

Figure B1. Example of the curves used at MWO.

Table B1. Droplet size distributions.

Fraction of LWC in each size group	*Distribution* (a/a_d)								
	A	*B*	*C*	*D*	*E*	*F*	*G*	*H*	*J*
0.05	1.00	0.56	0.42	0.31	0.23	0.18	0.13	0.10	0.56
0.10	1.00	0.72	0.61	0.52	0.44	0.37	0.32	0.27	0.194
0.20	1.00	0.84	0.77	0.71	0.65	0.59	0.54	0.50	0.42
0.20	1.00	1.17	1.26	1.37	1.48	1.60	1.73	1.88	2.20
0.30	1.00	1.00	1.00	1.00	1.00	1.00	1.00	1.00	1.00
0.10	1.00	1.32	1.51	1.74	2.00	2.30	2.64	3.03	4.00
0.05	1.00	1.49	1.81	2.22	2.71	3.31	4.04	4.93	7.34

ing the volume-median size K-value by the value of $(a/a_d)^2$ for that size group, since the droplet size is raised to the second power in the expression for K. The value of ϕ remains the same as for the volume-median size since droplet size does not appear in the expression for ϕ. The collection efficiency for each size group is then obtained from the curves of Brun et al. (1955) mentioned above. The weighted collection efficiency for each size group is obtained by multiplying the value in column three by the value in column five. The sum of column six is the overall weighted collection efficiency, giving the point $1/K = 0.01, E_M = 0.899$ for the $K\phi = 1000$ J curve.

This procedure differs from that of Langmuir and Blodgett (1946) in that the value of ϕ is held constant for each point, whereas in Langmuir and Blodgett ϕ was varied to keep $K\phi$ constant. The method of Brun et al. is correct, since ϕ is not a function of D.

Figure B1 shows an example of the curves used at MWO. All but a tiny fraction of exposures in natural wind will require only the curves for $K\phi = 20$, 200, and 1000.

Curve matching

Brun et al. (1955) give a rigorous exposition of the procedure for curve-matching and the determination of W and $C_{K=1}$. Briefly, the procedure can be explained by stating that the multiplication and division of numbers required for these determinations is equivalent to the addition and subtraction of the logarithms of those numbers, and this is done graphically by sliding the log-log graph of plotted points parallel to the theoretical curves, which are on the same type of log-log paper.

For a more intuitive understanding, note that the theoretical curves are asymptotic to the $E_M = 1$ axis for small values of $1/K$; the inverted T that you trace on your data plot is the location of that axis. Stating it another way, if your smallest cylinder had a collection efficiency of 100% ($E = 1$), its data point would have fallen on that axis and its EW value would have been equal to W.

Table B2. Sample calculation of E_M: $K\phi = 1000$, $K = 100$, distribution J.

1	*2*	*3*	*4*	*5*	*6*
Size group	$(a/a_d)^2$	*Fraction of water in size group*	*K*	*E*	*Weighted collection efficiency*
1	0.0031	0.05	0.31	0.087	0.0044
2	0.0377	0.10	3.77	0.715	0.0715
3	0.177	0.20	17.7	0.914	0.1828
4	1.00	0.30	100.0	0.972	0.2916
5	4.84	0.20	484.0	0.995	0.1990
6	16.00	0.10	1600.0	0.999	0.0999
7	54.0	0.05	5400.0	0.999	0.0500

Overall weighted collection efficiency, $E_M = 0.899$

Tab1e B3. Data for construction of theoretical curves.

		E_M								
$K\phi$	$1/K$	*A*	*B*	*C*	*D*	*E*	*F*	*G*	*H*	*J*
0	10	—	—	0.010	0.022	0.036	0.053	0.072	0.091	0.130
	4	0.051	0.069	0.085	0.107	0.126	0.146	0.167	0.186	0.221
	2	0.205	0.204	0.211	0.225	0.241	0.256	0.273	0.290	0.318
	1	0.380	0.374	0.373	0.379	0.384	0.389	0.395	0.402	0.413
	0.5	0.566	0.555	0.549	0.542	0.536	0.529	0.523	0.520	0.514
	0.2	0.789	0.768	0.750	0.732	0.713	0.695	0.679	0.668	0.643
	0.1	0.885	0.870	0.854	0.836	0.815	0.794	0.773	0.758	0.727
	0.05	0.932	0.925	0.918	0.898	0.885	0.867	0.846	0.828	0.798
	0.02	0.963	0.961	0.957	0.951	0.940	0.929	0.913	0.899	0.866
	0.01	0.978	0.976	0.977	0.972	0.965	0.958	0.946	0.934	0.905
20	10	—	—	0.0056	0.0137	0.0247	0.038	0.056	0.069	0.104
	4	0.038	0.052	0.067	0.085	0.103	0.122	0.142	0.161	0.197
	2	0.170	0.173	0.181	0.195	0.212	0.228	0.246	0.262	0.293
	1	0.342	0.340	0.341	0.346	0.354	0.362	0.370	0.376	0.389
	0.5	0.540	0.537	0.524	0.520	0.514	0.510	0.505	0.503	0.499
	0.2	0.780	0.759	0.739	0.721	0.698	0.682	0.667	0.655	0.632
	0.1	0.880	0.864	0.849	0.830	0.806	0.787	0.767	0.752	0.720
	0.05	0.930	0.921	0.913	0.898	0.882	0.865	0.842	0.827	0.796
	0.02	0.962	0.959	0.956	0.949	0.940	0.928	0.913	0.898	0.865
	0.01	0.978	0.976	0.974	0.971	0.966	0.957	0.946	0.934	0.905
200	10	—	—	0.0037	0.0092	0.0168	0.0269	0.040	0.054	0.086
	4	0.027	0.039	0.050	0.066	0.083	0.100	0.118	0.137	0.173
	2	0.135	0.138	0.146	0.165	0.182	0.196	0.216	0.229	0.261
	1	0.298	0.302	0.306	0.315	0.319	0.323	0.334	0.345	0.361
	0.5	0.493	0.486	0.482	0.480	0.477	0.474	0.471	0.472	0.471
	0.2	0.761	0.740	0.721	0.703	0.686	0.665	0.646	0.635	0.615
	0.1	0.874	0.859	0.846	0.826	0.805	0.777	0.754	0.739	0.705
	0.05	0.925	0.919	0.910	0.901	0.878	0.862	0.841	0.819	0.783
	0.02	0.960	0.959	0.955	0.948	0.938	0.927	0.911	0.894	0.866
	0.01	0.976	0.975	0.976	0.971	0.963	0.958	0.946	0.934	0.903
10^3	10	—	—	—	0.0066	0.0121	0.0193	0.028	0.039	0.066
	4	0.019	0.029	0.038	0.050	0.065	0.076	0.092	0.110	0.142
	2	0.109	0.109	0.122	0.138	0.154	0.164	0.181	0.199	0.231
	1	0.251	0.252	0.259	0.271	0.283	0.293	0.304	0.315	0.334
	0.5	0.460	0.452	0.423	0.447	0.447	0.438	0.437	0.438	0.440
	0.2	0.714	0.697	0.677	0.661	0.643	0.623	0.609	0.601	0.585
	0.1	0.830	0.816	0.800	0.783	0.763	0.743	0.724	0.711	0.683
	0.05	0.908	0.899	0.892	0.876	0.862	0.835	0.815	0.800	0.768
	0.02	0.953	0.953	0.949	0.943	0.933	0.912	0.896	0.882	0.851
	0.01	0.971	0.972	0.973	0.967	0.962	0.950	0.937	0.927	0.899
3×10^3	10	—	—	—	0.0041	0.0088	0.014	0.021	0.031	0.054
	4	0.013	0.020	0.027	0.039	0.048	0.060	0.075	0.088	0.120
	2	0.085	0.090	0.100	0.111	0.130	0.140	0.159	0.177	0.211
	1	0.218	0.225	0.235	0.244	0.251	0.256	0.268	0.282	0.303
	0.5	0.409	0.416	0.410	0.415	0.413	0.408	0.399	0.405	0.411
	0.2	0.687	0.668	0.652	0.641	0.623	0.601	0.591	0.583	0.567
	0.1	0.815	0.797	0.785	0.766	0.746	0.719	0.702	0.689	0.663
	0.05	0.884	0.878	0.867	0.855	0.839	0.813	0.795	0.779	0.750
	0.02	0.954	0.940	0.938	0.921	0.918	0.901	0.885	0.870	0.840
	0.01	0.968	0.966	0.970	0.964	0.954	0.940	0.927	0.917	0.888
10^4	10	—	—	—	—	—	0.0082	0.0136	0.0207	0.040
	4	0.008	0.013	0.017	0.023	0.034	0.046	0.059	0.073	0.103
	2	0.057	0.060	0.072	0.083	0.092	0.110	0.126	0.144	0.176
	1	0.157	0.163	0.172	0.188	0.202	0.216	0.231	0.246	0.272
	0.5	0.350	0.356	0.357	0.362	0.368	0.356	0.366	0.374	0.385
	0.2	0.645	0.630	0.615	0.599	0.591	0.559	0.550	0.542	0.533
	0.1	0.778	0.764	0.748	0.731	0.713	0.695	0.677	0.666	0.643
	0.05	0.865	0.857	0.849	0.830	0.816	0.793	0.777	0.762	0.734
	0.02	0.920	0.920	0.918	0.909	0.899	0.884	0.869	0.855	0.825
	0.01	0.952	0.950	0.955	0.946	0.939	0.930	0.918	0.907	0.879
10^5	10	—	—	—	—	—	—	—	—	—
	4	—	0.0045	0.0073	0.0110	0.00156	0.0202	0.0307	0.0391	0.061
	2	0.022	0.026	0.031	0.038	0.048	0.060	0.073	0.089	0.122
	1	0.080	0.086	0.094	0.109	0.125	0.140	0.156	0.171	0.200
	0.5	0.225	0.226	0.233	0.243	0.254	0.266	0.277	0.290	0.310
	0.2	0.485	0.479	0.474	0.470	0.465	0.463	0.462	0.463	0.460
	0.1	0.687	0.669	0.654	0.640	0.625	0.612	0.599	0.593	0.578
	0.5	0.805	0.794	0.782	0.768	0.750	0.734	0.719	0.706	0.681
	0.02	0.887	0.883	0.875	0.870	0.858	0.846	0.830	0.818	0.789
	0.01	0.930	0.926	0.924	0.920	0.913	0.904	0.891	0.880	0.855

APPENDIX C: STEP-BY-STEP PROCEDURE

The numbers in Table C1 are taken from an exposure made at MWO at 0332 on 7 Dec 1987. The value of w_i for a no. 3 cylinder has been changed to simulate an error in weighing. Some details of the procedure have been omitted, since they will depend on individual circumstances (exposure site, computer usage, etc.). One important service of this Appendix is to demonstrate the magnitude of the numbers you can expect to measure and compute; without such help it may be difficult to keep track of the decimal point since the unit of length is variously meters, centimeters, or micrometers.

Exposure

1. Make sure the instrument is dry and cold. If it has been cooled while still wet it may be impossible to disassemble it after the exposure, so check to see if all the parts move freely. Also check the exposure site and prepare to deploy your anemometer or deice a permanently mounted one.

2. Position the instrument for exposure and punch your stopwatch. Then, for a few moments, observe what's going on. Is the RMC rotating? If conditions are marginal, is water running down the smaller cylinders without freezing? (If so, give up and try again another day.) Check the progress of the run often enough to avoid excessive accumulation.

3. End the exposure when the deposit on the smallest cylinder has grown to approximately the original diameter of the next-larger one. Timing to within about five seconds is adequate. Bring the instrument back into the coldroom. Be careful; sooner or later you will probably be careless and break some ice or even one of the two smallest cylinders. (You should have spares for those small cylinders.) Place the instrument in a prepared position so that it stands securely upright. With your micrometer caliper, measure the diameters of the three smallest cylinders. If the collection is fragile rime, be careful not to crush it; adjust the micrometer by eye, not by feel. Remember to enter the duration time and all other measurements on your work sheet, and also indicate the character of the accumulation on each cylinder.

4. Put on a pair of cotton gloves, remove the smallest cylinder, measure the length of the collection to the nearest 0.05 cm, and weigh to the nearest 0.01 g. Repeat for the other cylinders, one at a time. If the ice is beginning to melt, weigh each cylinder before you measure its diameter. Diameters of the three largest ones are measured indirectly over a wire anvil (see last paragraph under *Instrumentation*). Separating the cylinders from the intercylinder adapters will be difficult if the collection is clear ice and you will have to develop your own technique, but see under *Exposure Procedure* for a suggestion.

Table C1. Sample exposure data and analysis.

Pressure (mb): 800 Temp (°C): −14 Wind speed (mph): 66
Exposure duration(s): 900 ρ_a (g/cm^3): 1.075×10^{-3}
V/η: 18.02×10^6 f_1: 187

Cylinder no.	*1*	*2*	*3*	*4*	*5*	*6*
C_i	0.462	0.758	1.33	—	—	—
m	—	—	—	0.586	0.560	0.568
C_o	0.158	0.502	1.11	—	—	—
C_o–b	—	—	—	1.738	3.955	7.115
C_{av}	0.310	0.630	1.22	2.32	4.52	7.68
L	9.20	10.25	7.35	7.40	7.35	7.40
w_i	2.84	19.46	8.08	21.31	42.13	78.88
w_o	1.84	17.64	5.79	18.90	39.72	77.03
EW	0.132	0.106	0.0962	0.0529	0.0273	0.0123

$C_{K=1}$ (cm): 2.9 W (g/m^3): 0.17
$K\phi$: 542 D_d (μm): 12
Curve used: 1000 Distribution: C
Points fitted: 5

Data reduction

5. Compute the average diameter C_{av} for each cylinder. For the three smallest ones this is simply equal to $(C_i + C_o)/2$. For the three largest cylinders, which were measured over an anvil, use the following expression:

$$C_{av} = m + (C_o - b)$$

where m = (anvil)+(cylinder wall)+(ice) and b = (anvil)+(cylinder wall).

6. Compute EW for each cylinder by eq 1 in body of this report (V in cm/s, L and C_{av} in cm).

7. Compute V/η and f_1 by eq 3 and 4. Note that temperature must be in kelvins (= °C+273, e.g., −14°C = 295 K).

8. On three-cycle log paper, plot the values of C_{av}

and EW, with C_{av} on the vertical axis and EW on the horizontal axis (Fig. 2a). (You will have to choose the values for the axes such that the plot will be near the center of the paper.)

9. Now for the curve-matching. You have to guess which family of theoretical curves to try first (usually $K\phi$ = 20, 200, or 1000). Say, for this example, that you pick the 200 family. Keeping the axes parallel, slide your plotted graph around on the theoretical curves until you find the best fit (in this case the C curve). You will see an inverted T on the theoretical curve, labeled C, with its horizontal arm on the $1/K = 1$ axis. Note that this is under the value $C_{av} = 2.5$ on your plot, meaning that $C_{K=1} = 2.5$. Multiply this value by the value of f_1 which you found in Step 7 (2.5×187 = 468). Determine whether 468 is closer to 200 than it is to 1000, on a logarithmic scale (you can use the scale on the graph paper for this). The answer is "no," it's closer to 1000. This means that you must repeat the matching on the $K\phi$ = 1000 curves.

10. Do your final curve-matching on the 1000 curves and you will find that the best fit is again on the C curve. Lightly trace the curve through your plotted points and also trace the inverted T labeled C. (Its location will be slightly different from what it was when you tried the 200 curve.) Read the value of the horizontal arm of the T on your graph ($C_{K=1} = 2.9$). Then read the value of the vertical arm of the T on your graph ($EW_{E=1} = 0.17$). This means that the liquid-water content (LWC) for your exposure was 0.17 g/m.

11. Multiply your value of $C_{K=1}$ by f_1 to find the value of $K\phi$. Calculate the value of D_d by eq 5. In the space for "Distribution" on your analysis sheet, enter C, and indicate the number of data points which fit the theoretical curve within 5%.

Important note: It is essential that the theoretical curves be on the same type of graph paper which you use for your plots of C_{av} vs EW. You must construct your own curves from the values given in Table B3. It is important to use three-cycle by three-cycle paper with as large a format as practicable. Construction requires skillful use of french curves.

REPORT DOCUMENTATION PAGE

Form Approved
OMB No. 0704-0188

1. AGENCY USE ONLY (Leave blank)	2. REPORT DATE	3. REPORT TYPE AND DATES COVERED
	January 1991	

4. TITLE AND SUBTITLE

Rotating Multicylinder Method for the Measurement of Cloud Liquid-Water Content and Droplet Size

5. FUNDING NUMBERS

PE: 4A161102AT24 ✓
TA: FS
WU: 005

6. AUTHORS

John B. Howe

7. PERFORMING ORGANIZATION NAME(S) AND ADDRESS(ES)

Mount Washington Observatory
Gorham, New Hampshire 03581

8. PERFORMING ORGANIZATION REPORT NUMBER

9. SPONSORING/MONITORING AGENCY NAME(S) AND ADDRESS(ES)

Sponsor:
Office of the Chief of Engineers
Washington, D.C. 20314-1000

Monitor:
U.S. Army Cold Regions Research and Engineering Laboratory
72 Lyme Road
Hanover, New Hampshire 03755-1290

10. SPONSORING/MONITORING AGENCY REPORT NUMBER

CRREL Report 91-2

11. SUPPLEMENTARY NOTES

12a. DISTRIBUTION/AVAILABILITY STATEMENT

Approved for public release; distribution is unlimited.

Available from NTIS, Springfield, Virginia 22161.

12b. DISTRIBUTION CODE

13. ABSTRACT (*Maximum 200 words*)

Since its development at the Mount Washington Observatory in the 1940s the rotating multicylinder (RMC) method has been the simplest, most reliable, and usually the most accurate means of measuring the liquid-water content and droplet size in clouds and fog. The development history of the method is reviewed in this report. Fabrication of the instrument, exposure and data-reduction techniques, and the underlying theory of the method are described in detail. Accuracy of the RMC method is discussed and comparison tests with other instruments are briefly reviewed.

14. SUBJECT TERMS

Clouds
Cold regions metecrology
Droplet size
Liquid water contet
Rotating multicylinder method

15. NUMBER OF PAGES

21

16. PRICE CODE

17. SECURITY CLASSIFICATION OF REPORT	18. SECURITY CLASSIFICATION OF THIS PAGE	19. SECURITY CLASSIFICATION OF ABSTRACT	20. LIMITATION OF ABSTRACT
UNCLASSIFIED	UNCLASSIFIED	UNCLASSIFIED	UL

NSN 7540-01-280-5500

U.S. GOVERNMENT PRINTING OFFICE 1991-500-063 22068

Standard Form 298 (Rev. 2-89)
Prescribed by ANSI Std. Z39-18
298-102